Int. J. Electrochem. Sci., 3 **(2008)** 1364 - 1385

International Journal of ELECTROCHEMICAL SCIENCE
www.electrochemsci.org

Spatiotemporal Oscillations in Biological Molecules: Hydrogen Peroxide and Parkinson's Disease

C. V. Krishnan[1,2,*], *M. Garnett*[1] *and B. Chu*[2]

[1] Garnett McKeen Lab, Inc., 7 Shirley Street, Bohemia, NY 11716-1735, USA
[2] Department of Chemistry, Stony Brook University, Stony Brook, NY11794-3400, USA
[*]E-mail: ckrishnan@notes.cc.sunysb.edu

Received: 18 September 2008 / *Accepted:* 12 October 2008 / *Published:* 17 November 2008

Oxidative stress, due to excessive reactive oxygen species such as H_2O_2, is implicated in the pathogenesis of Parkinson's disease. The electronic behavior of this molecule in the presence of the most common biological electrolyte, sodium chloride, has been investigated by frequency response analysis. H_2O_2 exhibited negative differential resistance or impedance in the first and second quadrants, a characteristic of tunnel diode behavior. With increasing concentration of H_2O_2, there was a shift to slightly more negative potentials at which the impedance spectra exhibited negative real impedance. This finding was in agreement with the observations of a slight cathodic shift in the cyclic voltammetric peak. When the potential was changed from the most cathodic to less and less cathodic, the impedance spectral characteristics changed from capacitive loops to impedance in two quadrants and then back to capacitive loops. In the range of potentials at which negative differential resistance was observed, there was a fixed potential at which the frequency was the highest when the impedance became negative. At this potential, the higher the H_2O_2 concentration, the higher the frequency at which the real part of the impedance became negative. Depending on the potential and concentration of H_2O_2, negative real impedance was observed at frequencies in the range 260 Hz – 40 mHz. The variations in impedance data were higher in 0.04 M NaOH compared to that in near neutral solutions. Insignificant influence of 1 or 2 mM chloride on the impedance spectra in highly basic solution was observed. Negative differential resistance was also observed for 88 mM H_2O_2 in solutions of 0.10 M $NaClO_4$ and 0.10 M Na_2SO_4. The results suggested that the electronic character of H_2O_2 could be dictated by the potential, bulk electrolyte concentration, pH, and the concentration of H_2O_2. To explain our admittance data, we have introduced the concept of "potential induced and peroxide-mediated" ion pair formation between sodium and chloride ions in a way similar to our earlier concept, "potential induced and water-structure-enforced" ion pair formation. Our results demonstrate the need for multiple electrodes at multiple locations with tunable frequencies and voltages for possible treatment of Parkinson's disease by deep brain stimulation because of the variations in the concentration of H_2O_2 at different locations and at different times and consequent subtle changes in its electronic properties.

Keywords: Parkinson's disease, electronic properties of hydrogen peroxide, spatiotemporal oscillations, tunnel diode, admittance.

1. INTRODUCTION

Parkinson's disease is a slow, progressive neurological disorder. It is characterized by the loss of dopaminergic neurons in the pars compacta of the substantia nigra. While the causes for degeneration of these neurons are not well understood, dopaminergic neurons in patients with Parkinson's disease are thought to be vulnerable to oxidative stress, due to excessive reactive oxygen species [1-6].

A major source of reactive oxygen species, such as superoxide anion, hydroxyl radical, hydrogen peroxide, and singlet oxygen is the mitochondria and these neurons contain a large number of mitochondria. Cells have been naturally gifted with various enzymatic antioxidants, such as superoxide dismutase, catalase, and glutathione peroxidase and non- enzymatic antioxidants, such as glutathione, to protect them from oxidative damage [7]. However, a fraction evades this cellular defense and causes permanent or transient damage to proteins, lipids and nucleic acids of the cell. Electron leakage from the electron transport chain complexes during normal respiration causes the production of reactive oxygen species. There are about nine known sources of reactive oxygen species in mitochondria [8]. In particular, complex I and complex III are the primary sites of reactive oxygen species production [9-11]. In Parkinson's disease, mitochondrial dysfunction is evident from 30 to 40 percent decrease in complex I activity in the substantia nigra pars compacta [12]. The mitochondria themselves are targets of their own oxidant by-products and are more vulnerable, compared to the other organelles. This leads to decreased electron transport, increased free radical production, and increased mitochondrial damage [13].

Before the discovery of levodopa, one common treatment to arrest tremor in patients with Parkinson's disease was high frequency stimulation (> 100 Hz) of the thalamic ventral intermediate nucleus [14, 15]. The electrical signals that cause the Parkinson's disease symptoms are blocked by these impulses. The impetus for the development of the modern deep brain stimulation was the side effects as well as the limits of chronic levodopa treatment. Levodopa is also known to produce free radicals during its normal metabolism. In the deep brain stimulation treatment, the neurostimulator delivers tiny electrical impulses that interfere with and block the electrical signals (abnormal nerve signals) from targeted areas in the brain that cause the symptoms of the Parkinson's disease.

Progressive reduction of O_2 produces $O_2^{\cdot-}$, H_2O_2, and finally $^{\cdot}OH$ along with OH^-. The hydroxyl radical can lead to lipid peroxidation and alter the structural integrity of neural membranes. Excess Fe^{2+}, also found in patients with Parkinson's disease, can reduce peroxide and produce $^{\cdot}OH$. Dopamine undergoes auto-oxidation, producing $^{\cdot}OH$, H_2O_2, semiquinone radical and finally a quinone. Enzymatic metabolism of dopamine also produces H_2O_2 [1].

While H_2O_2 seems to have a deleterious effect in patients with Parkinson's disease, recent experiments suggest some beneficial aspects of this molecule. It reacts with thiol residues and acts as a switch in signaling pathways. For example peroxide mediated cellular signaling is suggested through oxidation of cysteine residues in peroxoredoxins to sulfenic acid. Further oxidation of cysteine-sulfenic acid produces cysteine-sulfinic acid, which inactivates the enzyme. While at low concentrations, H_2O_2 serves as an intracellular messenger, at higher concentrations and on prolonged exposure, H_2O_2

induces cell death by both apoptosis and necrosis. The effects of H_2O_2 on cellular messenger systems have been summarized elegantly [16].

In neutrophils, millimolar quantities of H_2O_2 are produced for the purpose of microbial killing. Thus H_2O_2 serves different roles, good and bad, in our daily life.

Past electrochemical impedance measurements of hydrogen peroxide have been concentrated on the oscillatory behavior at high concentrations and at high acidities [17-21]. Current oscillations have also been observed during H_2O_2 reduction in alkaline solutions [22-26]. The electrodes used for many of these investigations include Pt, Ag, Au(100) and semiconductor electrodes p-$CuInSe_2$ and n-GaAS.

The purpose of the present investigation is to bring focus on the electronic properties of this unique molecule, H_2O_2. In our previous investigation using cyclic voltammetry, we have demonstrated that the 'autocatalytic' H_2O_2 reduction process is sensitive to the range of the sweep potential, concentration of H_2O_2, NaCl concentration, and pH. We have also discussed the complexity of the multiple equilibria involved in H_2O_2 redox processes. Biological processes become even more complicated because of the ready availability of numerous enzymes and metal redox centers. We have focused our attention on the oscillatory behavior at low concentrations of H_2O_2 in the presence of the most common biological electrolyte, sodium chloride, and around neutral pH. It is increasingly evident that cell signaling takes place when there is a rapid increase or burst in the concentration of H_2O_2. In order to probe this, we have also investigated the effects of concentration of H_2O_2 on its electronic properties.

2. EXPERIMENTAL PART

The EG &G PARC Model 303A SMDE trielectrode system (mercury working electrode, platinum counter electrode and Ag/AgCl saturated KCl reference electrode) along with Autolab ecochemie was used for electrochemical impedance measurements.

Analytical grade salts, J.T. Baker 31.3% H_2O_2, and distilled water were used for all the experiments. H_2O_2 was standardized by titration in the presence of 1 M H_2SO_4 with standard potassium permanganate. Solutions were purged with N_2 before experiment. Variations of pH were carried out using 1 M HCl or 1 M NaOH.

Impedance measurements were carried out in the range 1000Hz to 30 mHz. The amplitude of the sinusoidal perturbation was 10 mV.

3. RESULTS AND DISCUSSION

3.1. Admittance

3.1.1. Potential induced and peroxide-mediated ion pair formation

The admittance data at 1000 Hz for 0.10 M NaCl, 0.10 M $NaClO_4$ and 0.10 M Na_2SO_4 in the absence and presence of 88 mM H_2O_2 are shown in Figures 1a, 1b, and 1c. Their comparison data in the presence of the three electrolytes are shown in Figure 1d. The admittance data for 0.10 M NaCl in the absence and presence of 88 mM H_2O_2 at other frequencies are shown in Figures 2a and 2b and their comparison data in Figure 2c.

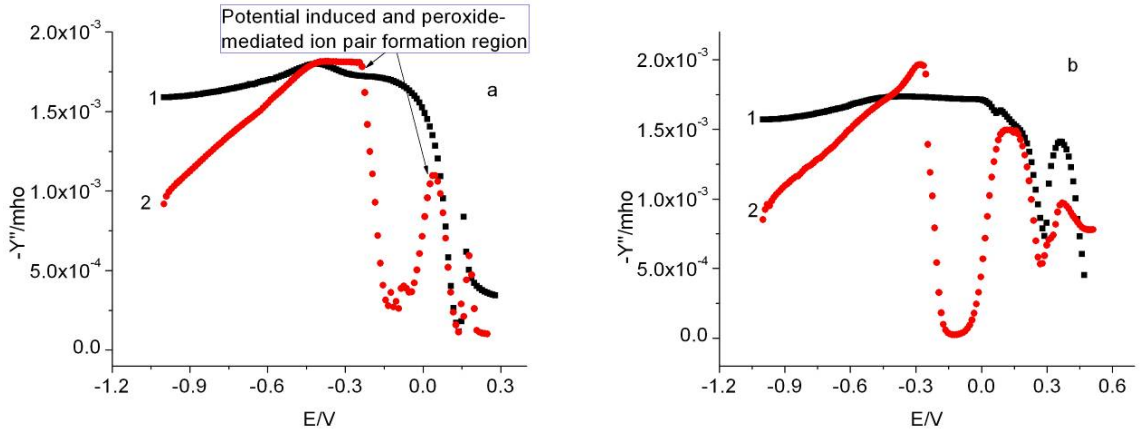

Figures 1a, 1b Admittance comparison of a) 0.10 M NaCl, pH ~ 6.0, 1000 Hz, 1) no H_2O_2 2) in the presence of 88 mM H_2O_2 ; b) 0.10 M $NaClO_4$, pH ~ 6.0, 1000 Hz, 1) no H_2O_2 2) in the presence of 88 mM H_2O_2

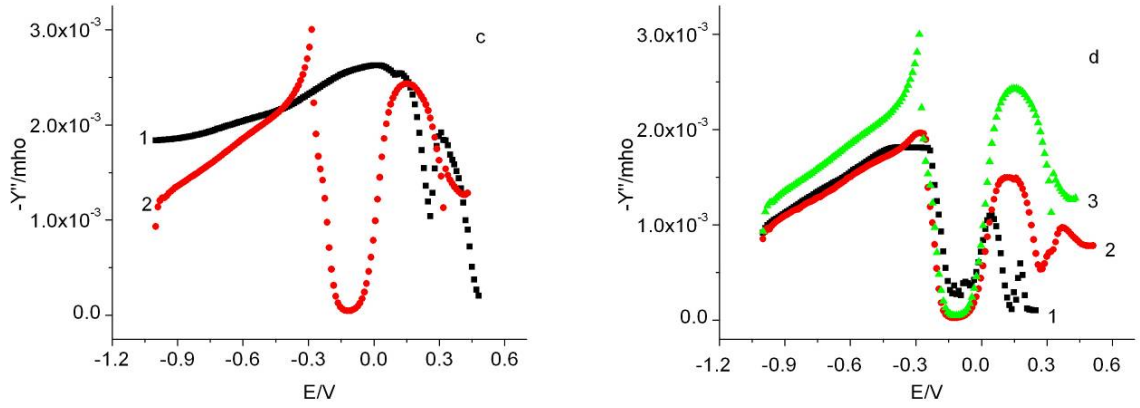

Figures 1c, 1d Admittance comparison of c) 0.10 M Na_2SO_4, pH ~ 6.0, 1000 Hz, 1) no H_2O_2 2) in the presence of 88 mM H_2O_2 ; d) in the presence of 88 mM H_2O_2 and 1) 0.10 M NaCl 2) 0.10 M NaClO4 3) 0.10 M Na_2SO_4

The nature of the admittance data for H_2O_2 was very similar in the presence of the three electrolytes. However, there were major differences in the absence and presence of H_2O_2. We had recently reported admittance data for aqueous solutions of sodium halides at different concentrations [27]. In order to explain the admittance behavior at potentials close to 0.0 V and the concentration effects, we had introduced the new concept of 'potential induced and water structure-enforced ion pair formation' between sodium and halides ions [27]. When the potential sweep changed from -1.0 V to

less and less cathodic potentials and then to positive potentials, the orientation of the ions towards mercury at or near the double layer also changed from that of Na^+ to Cl^- or other halide ions. Also the corresponding orientation of water changed from that of hydrogen to oxygen pointing towards the mercury electrode. During this changeover process, if there were considerable hydrogen bond breaking, it would result in an admittance increase. If there was a cooperative process between the sodium ion and the halide ion with or without an intervening water molecule, the ion pair formed should decrease the admittance. This concept could explain all the data for sodium halides at all frequencies. The increase in admittance at potentials close to 0.0 V at low frequencies and the sudden decrease after the maxima before the beginning of passivation, as shown in Figure 2a could be explained by this concept.

We had also recently reported cyclic voltammetric data for H_2O_2 in the presence of these electrolytes [28]. The data could be explained by 'normal' and 'activated' or 'autocatalytic' H_2O_2 reduction processes at more cathodic and less cathodic potentials, respectively. The explanations for the cyclic voltammetric data were consistent with that observed for 20 mM H_2O_2 in 0.1 M $HClO_4$ using polycrystalline silver electrode [20].

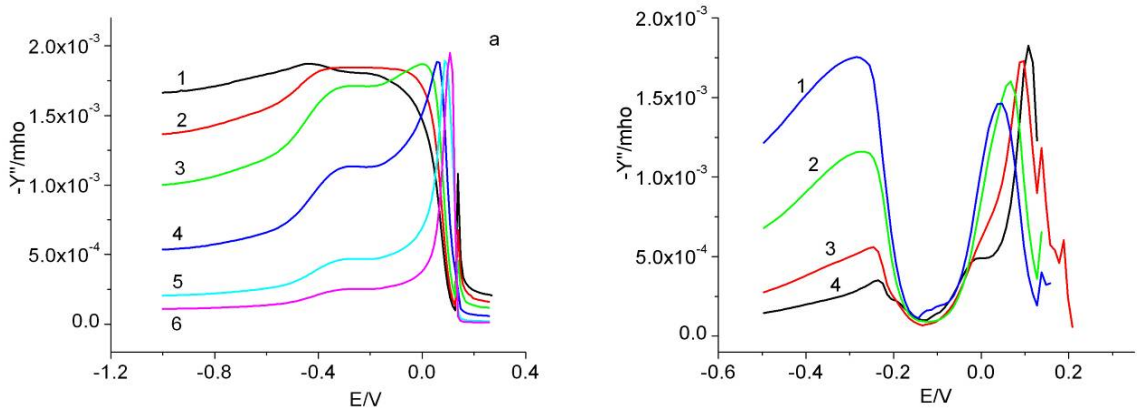

Figure 2a, 2b Admittance of a) 0.10 M NaCl, pH ~6.0, 1) 1000 Hz 2) 750 Hz 3) 500 Hz 4) 250 Hz 5) 100 Hz 6) 50 Hz ; b) 0.10 M NaCl and 88 mM H_2O_2, pH ~ 6.0, 1) 500 Hz 2) 250 Hz 3) 100 Hz 4) 50 Hz

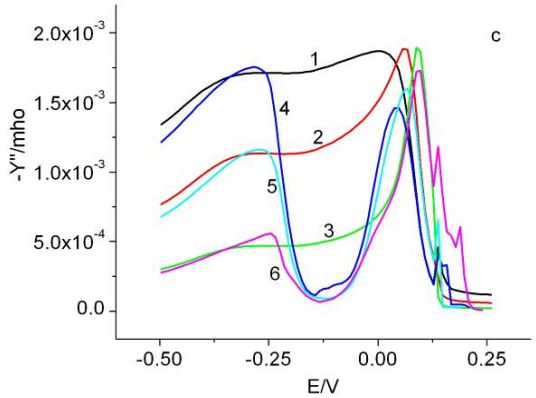

Figure 2c Admittance comparison of 0.10 M NaCl, pH 5.25 1) 500 Hz 2) 250 Hz 3) 100 Hz and 0.10 M NaCl and 88 mM H_2O_2, pH ~ 6.0 4) 500 Hz 5) 250 Hz 6) 100 Hz

The data at most cathodic potentials, as shown in Figures 1 and 2, correspond to the 'normal' H_2O_2 reduction region. These data were very similar to the data without any H_2O_2 except that the admittance was slightly less in the presence of H_2O_2 and the decline in admittance was steeper at most cathodic potentials, similar to the cathodic reduction current in cyclic voltammetry [28].

The major difference in admittance in the absence and presence of H_2O_2 was in the region of 'activated' or 'autocatalytic' H_2O_2 reduction region. A careful examination of the data in Figure 1a showed that there was a sudden decrease in admittance around -0.3 V followed by a gradual increase to about 0.0 V. The admittance decreased again after about 0.0 V and merged with the NaCl curve.

In order to explain this part of the admittance curve around the region of 'autocatalytic' H_2O_2 reduction, we are introducing another new concept, "potential induced and peroxide-mediated ion pair formation" between Na^+ and Cl^- ions. This is very similar to the concept we had introduced, "potential induced and water structure-enforced ion pair" formation between Na^+ and Cl^- ions [27]. Our reasoning for this introduction is as follows.

Hydrogen peroxide has a skewed chain structure and its dielectric constant at 25^{o}C increases from 93 for the pure liquid to 120 for a 65 % solution [29]. The liquid is more highly associated than H_2O via hydrogen bonding. The dipole moment of hydrogen peroxide of 2.26 Debye units is much higher than that of pure water. Even though numerous electrochemical investigations of H_2O_2 have been carried out in highly acidic and basic solutions, we are not aware of any investigations detailing its double layer behavior. There is no reason why H_2O_2 should not compete with H_2O for ion-dipole interactions. Depending on the concentration of H_2O_2 in the solution, there will be oriented H_2O molecules as well as H_2O_2 molecules around Na^+ and Cl^- or other negative ions. The hydrogen bond breaking effects as well as cooperative ion pair formation between Na^+ and Cl^- with an intervening H_2O_2 or H_2O molecule is also possible during the gradual change in potential from cathodic to less cathodic and finally to anodic potentials when the orientation of the ion towards mercury also changes from Na^+ to Cl^-. The merging of the two admittance curves, in the presence and absence of H_2O_2, after about 0.0 V demonstrates the stronger influence of H_2O_2 compared to that of H_2O. The region of this ion pair formation is also the 'activated' or 'autocatalytic' H_2O_2 reduction region.

This region of ion pair formation is nearly the same for 0.10 M NaCl, $NaClO_4$ or Na_2SO_4 as shown in Figure 1d. In all the three cases, the admittance was less in the presence of H_2O_2 in the extreme cathodic region of normal H_2O_2 reduction. Also the interaction between the ions and H_2O_2 were stronger than with H_2O.

3.1.2. Influence of pH on the potential induced and peroxide-mediated ion pair formation

The influence of pH on the formation of these ion pairs was investigated at two different frequencies of 1000 and 500 Hz and these data are shown in Figure 3. The moderate pH changes did not have any significant influence on this region of 'potential induced and H_2O_2 mediated' ion pair formation

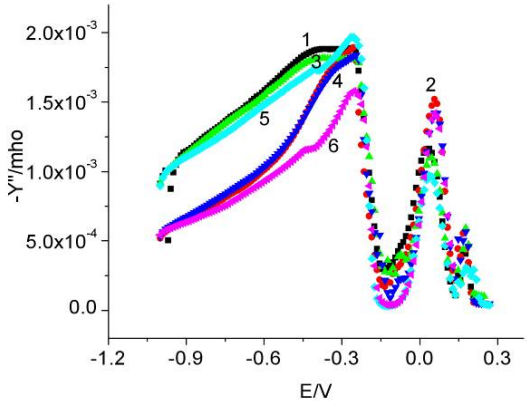

Figure 3. Admittance data for 0.1M NaCl, 88 mM H_2O_2, 1000 Hz, 1) pH 3.05 3) pH 5.72 5) pH 9.28; 500 Hz, 2) pH 3.05 4) pH 5.72 6) pH 9.28; pH adjusted with NaOH and HCl

3.1.3. Influence of H_2O_2 concentration on the potential induced and peroxide-mediated ion pair Formation

The admittance data at 1000 Hz for a constant 0.10 M NaCl in the presence of 0.88 mM, 8.8 mM, 17.6 mM, 88 mM and 352 mM H_2O_2 are shown in Figure 4a. With an increase in the concentration of H_2O_2, there was a cathodic shift in the region where the potential induced and peroxide-mediated ion pair formation between Na^+ and Cl^- began. All the curves merged with the 0.10 M NaCl data without any peroxide around 0.1 V. This region of ion pair formation became wider and wider with an increase in the concentration of H_2O_2 and was consistent with our observation with the cyclic voltammetric data [28].

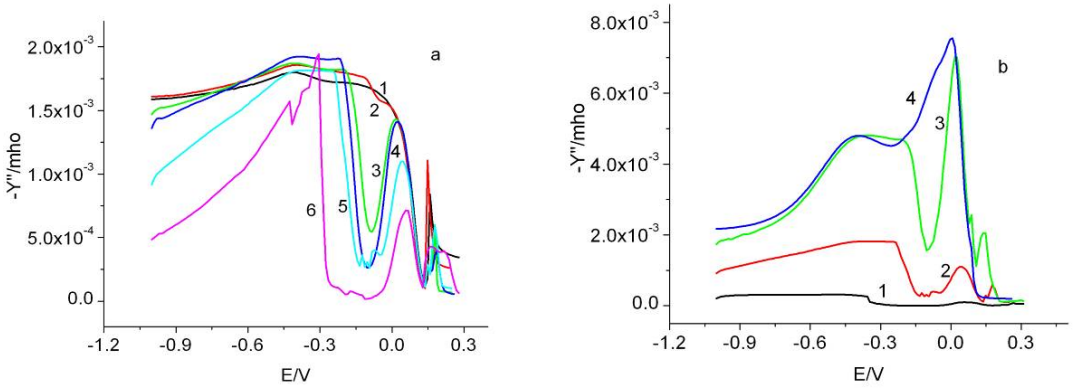

Figures 4a, 4b Admittance comparison of a) 0.10 M NaCl, pH ~ 6.0 in H_2O_2 1) 0.0 mM 2) 0.88 mM 3) 8.8 mM 4) 17.6 mM 5) 88 mM 6) 352 mM; 1000 Hz; b) 88 mM H_2O_2 in NaCl 1) 0.02 M 2) 0.10 M 3) 1.0 M 4) 1.0 M but without H_2O_2

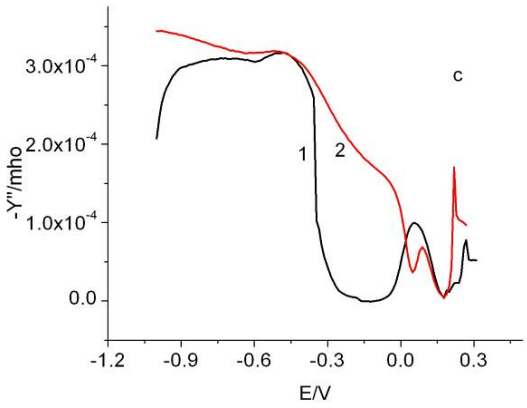

Figure 4c Admittance comparison of 0.02 M NaCl, pH ~ 6.0 in H_2O_2 1) 88 mM 1) 0.0 mM; 1000 Hz

3.1.4. Influence of NaCl concentration on the potential induced and peroxide-mediated ion pair Formation

At a constant 88 mM H_2O_2 concentration, the concentration of NaCl was varied from 0.02 M to 0.10 M and 1.0 M, with the results being shown in Figure 4b. To see the data more clearly, the data for 0.02 M NaCl with and without 88 mM H_2O_2 are shown in an expanded scale in Figure 4c. We had reported before that the potential induced and water structure-enforced ion pair formation was better at lower concentrations of NaCl [27] and a similar behavior was exhibited by potential induced and peroxide-mediated ion pair formation as evidenced by the cathodic shift which was in the order 0.02 M > 0.10 M > 1.0 M. This region of ion pair formation around -0.3 to 0.0 V also became narrower with increasing concentration of NaCl. In all the three cases the curves merged with the respective pure NaCl concentration near the region of passivation.

3.2. Differential Capacitance

The differential capacitance data for 88 mM H_2O_2 in 0.10 M NaCl at various frequencies are shown in Figure 4a. The data for 1000 Hz and 500 Hz are replotted in Figure 4b along with that of pure NaCl. In the absence of Faradaic reactions, the double layer capacitance was expected to be independent of frequency when obtained from differential capacitance measurements after compensating for ohmic resistance. We had not observed any frequency dispersion for 0.01, 0.10 and 1.0 M NaCl [27] in the potential range 0.0 to -1.0 V. There was practically no dispersion near the region of passivation, curves 1 and 2, in Figure 4b for pure NaCl. In the presence of 88 mM H_2O_2 we observe some dispersion at extreme cathodic potentials, especially at frequencies below 500 Hz (curves 5 and 6, Figure 4a) was detected. This is consistent with the fact that 'normal' H_2O_2 reduction takes place in this region. In the 'activated' or 'autocatalytic' H_2O_2 reduction region at less cathodic potentials, a much higher frequency dependence at frequencies below 500 Hz was observed. A cathodic peak followed by a shoulder at still less cathodic potential was observed at higher frequencies. The shoulder seemed to grow when the frequency was lowered and merged into one peak

at the lowest frequencies explored. We had truncated the data in Figure 4a after the shoulder for clarity.

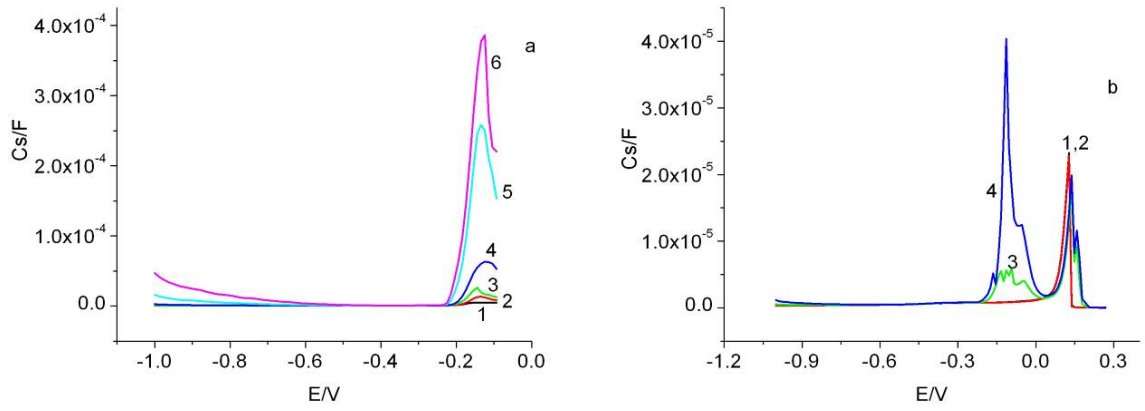

Figures 5a, 5b Capacitance of a) 88 mM H_2O_2 in 0.10 M NaCl, pH ~ 6.0, 1) 1000 Hz 2) 750 Hz 3) 500 Hz 4) 250 Hz 5) 100 Hz 6) 50 Hz; b) 0.10 M NaCl, pH ~ 6.0, 1) 1000 Hz 2) 500 Hz; in the presence of 88 mM H_2O_2 3) 1000 Hz 4) 500 Hz

Another interesting observation was that the capacitance peak potential did not match the major 'autocatalytic' H_2O_2 reduction peak. Instead it seemed to match the cathodic peak during the reverse scan from -1.0 V in the positive direction. Similar to the observation here we had observed a shoulder cathodic peak in the cyclic voltammetry data. The minor anodic shift observed for the mercury-chloride interaction in the presence of H_2O_2 was observed here in the capacitance data also at potentials close to the passivation region. A doublet was observed instead of a single peak in the presence of H_2O_2.

3.3. Nyquist plots

3.3.1. Influence of NaCl concentration

At a fixed 88 mM H_2O_2 concentration, the influence of NaCl was investigated, as shown in Figures 6-8. When the potential was changed from the most cathodic to less and less cathodic, the impedance behavior exhibited changed from a capacitive loop to impedance in two quadrants, where the real impedance became negative. The frequency at which the real impedance became negative also became higher and higher. At still higher potentials (but cathodic), the impedance exhibited capacitive loops again.

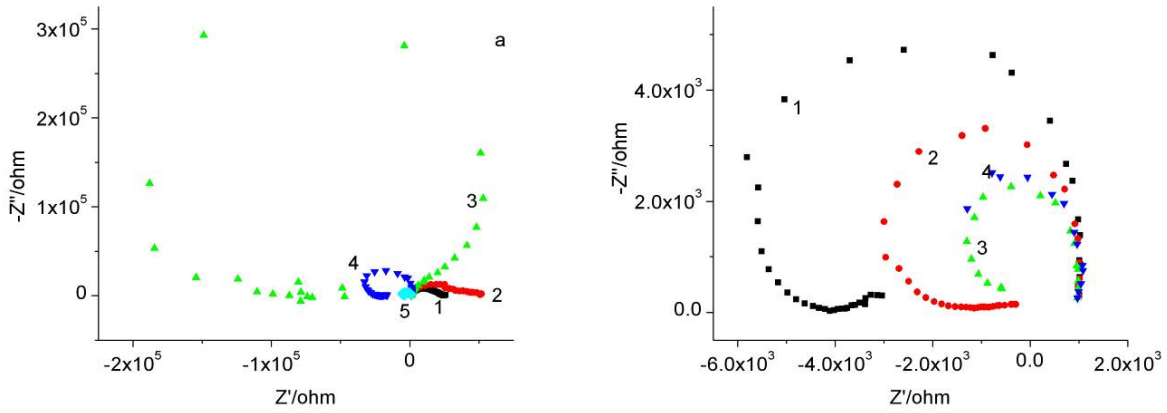

Figures 6a, 6b Nyquist plots for 0.02 M NaCl, 88 mM H_2O_2 at a) 1) -0.43 V 2) -0.42 V 3) -0.41 V 4) -0.40 V 5) -0.37 V; b) 1)-0.37 V 2) -0.34 V 3) -0.31 V 4) -0.28 V The real impedance becomes negative at 1.745 Hz (-0.41 V), 19.71 Hz (-0.40 V), 78.9 Hz (-0.37 V), 98.6 Hz (-0.34V), 98.6 Hz (-0.31 V), 98.6 Hz (-0.28 V)

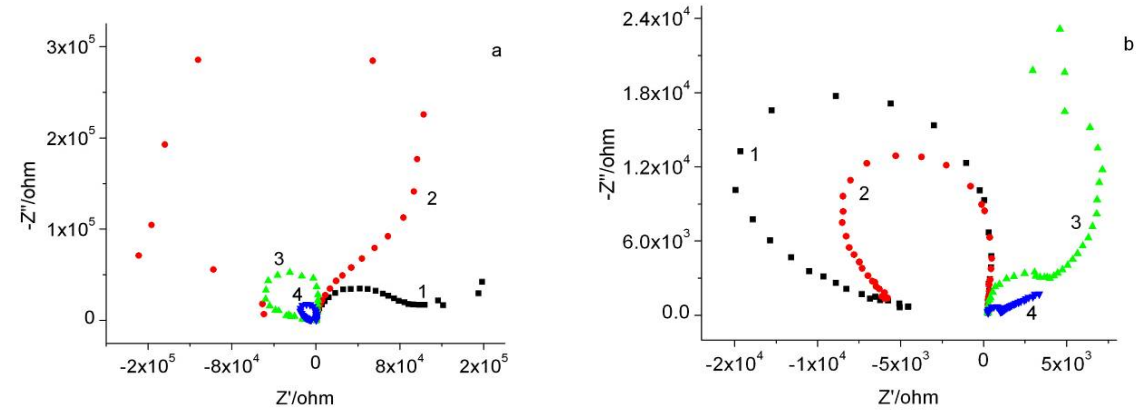

Figures 7a, 7b Nyquist plots for 0.1 M NaCl, 88 mM H_2O_2 at a) 1) -0.31 V 2) -0.28 V 3) -0.25 V 4) -0.22 V; b) 1)-0.22 V 2) -0.19 V 3) -0.16 V 4) -0.13V The real impedance becomes negative at 226.9 mHz (-0.28 V), 3.72 Hz (-0.25 V), 17.92 Hz (-0.22 V), 17.92 Hz (-0.19V)

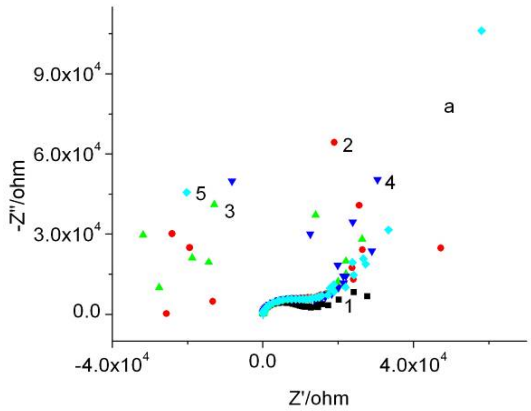

Figure 8. Nyquist plots for 1.0 M NaCl, 88 mM H_2O_2 at a) 1) -0.25 V 2) -0.22 V 3) -0.20 V 4) -0.19 V 5) -0.18 V; The real impedance becomes negative at 82 mHz (-0.22 V), 106 mHz (-0.20 V), 64 mHz (-0.19 V), 39 mHz (-0.18V)

The data in Figures 6-8 indicated that the exhibition of negative differential resistance, a characteristic of tunnel diode behavior is sensitive to the concentration of NaCl at fixed H_2O_2 concentration. The frequency at which the real part of the impedance becomes negative is controlled by the applied potential. The data points at which the real part of the impedance became negative at the highest frequencies were 98.6 Hz, 17.92 Hz and 106 mHz at 0.02, 0.10 and 1.0 M NaCl respectively, for 88 mM H_2O_2. The figures also indicate that the curve is smoother for 0.02 M NaCl and more chaotic for 1.0 M NaCl. The anodic shift in the best potential with the highest frequency for the real part of impedance to become negative was greater with increasing concentration of NaCl. This anodic shift was also observed in the cyclic voltammetric data we had reported in the preceding paper [28].

3.3.2. Influence of H_2O_2 concentration

At a fixed 0.10 M NaCl concentration, the influence of H_2O_2 on the impedance behavior was investigated. Typical results for 0.88, 8.8 and 352 mM H_2O_2 are shown in Figures 9-10. The real impedance became negative for 0.88 mM H_2O_2, at 39 mHz (-0.19 V), 378 mHz (-0.15 V), 487 mHz (-0.13 V), 487 mHz (-0.11V); for 8.8 mM H_2O_2 at 227 mHz (-0.28 V), 3.72 Hz (-0.25 V), 17.92 Hz (-0.22 V), 17.92 Hz (-0.19 V); for 17.6 mM H_2O_2 at 136 mHz (-0.31 V), 1.35 Hz (-0.28 V), 8.21 Hz (-0.25 V), 19.71 Hz (-0.22 V), 8.21 Hz (-0.19 V); for 88 mM H_2O_2 at 226.9 mHz (-0.28 V), 3.72 Hz (-0.25 V), 17.92 Hz (-0.22 V), 17.92 Hz (-0.19V); and for 352 mM H_2O_2, at 65.7 Hz (-0.40 V), 98.6 Hz (-0.35 V).

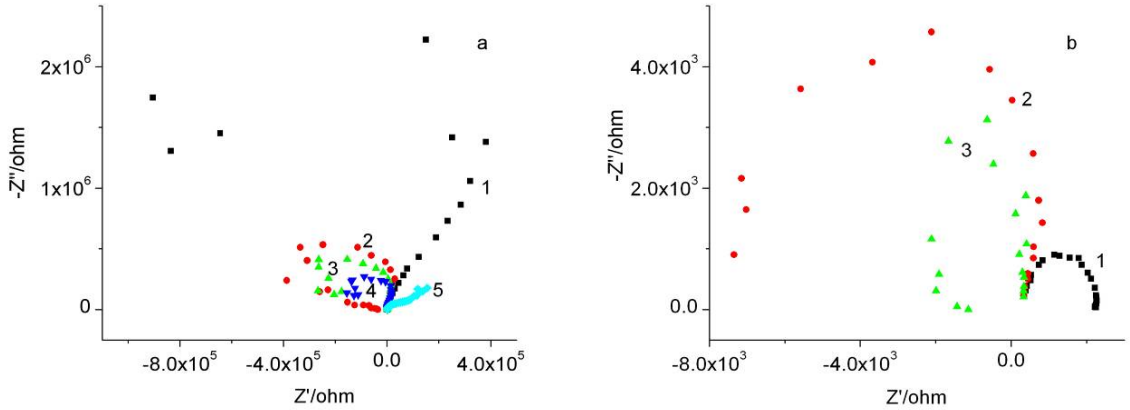

Figures 9a, 9b Nyquist plots for a) 0.10 M NaCl, 0.88 mM H_2O_2 at 1) -0.19 V 2) -0.15 V 3) -0.13 V 4) -0.11 V 5) -0.08 V; b) 0.10 M NaCl, 352 mM H_2O_2 at 1) -0.45 V 2) -0.40 V 3) -0.35 V.

The impedance data became more chaotic at low frequencies with 352 mM H_2O_2. A comparison of Figures 7, 9, and10 indicated the electronic behavior to be very smooth at concentrations above 10 mM. It is also interesting to note that impedance in two quadrants is exhibited even at concentrations less than 1 mM H_2O2.

With increasing concentration of H_2O_2, there was a cathodic shift in the potential at which the real impedance became negative. This is consistent with the cyclic voltammetric data reported in our previous communication [28].

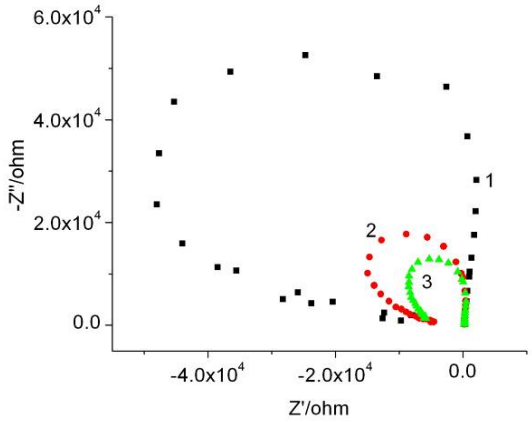

Figure 10. Nyquist plots for 0.10 M NaCl, 8.8 mM H_2O_2 at 1) -0.25 V 2) -0.22 V 3) -0.19 V.

3.3.3. Influence of Anion

Impedance measurements with 0.10 M $NaClO_4$ and 0.10 M Na_2SO_4 in the presence of 88 mM H_2O_2 exhibited similar behavior to that of NaCl. For $NaClO_4$, the real impedance became negative at 2.24Hz (-0.34 V), 39.4 Hz (-0.31 V), 78.9 Hz (-0.28 V), 78.9 Hz (-0.25 V), 78.9 Hz (-0.22 V), 49.3 mHz (-0.19 V). For Na_2SO_4, the real impedance became negative at 8.21Hz (-0.34 V), 39.4 Hz (-0.31 V), 65.7 Hz (-0.28 V), 131.4 Hz (-0.25 V), 106 mHz (-0.22 V). A comparison of $NaClO_4$ and Na_2SO_4 impedance behavior at two potentials, -0.28 and -0.25 V, where they exhibited the highest frequency at which the real impedance became negative, is shown in Figure 11. The data suggested better electronic character for Na_2SO_4 compared to that of $NaClO_4$. It was not possible to arrive at this information from admittance data. However our cyclic voltammetric data indicated that the catalytic activity for both the 'normal' and 'activated' or 'autocatalytic' H_2O_2 reduction was the highest for sulfate and least for perchlorate [28].

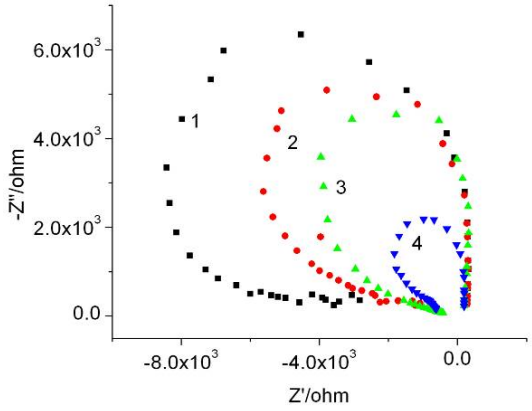

Figure 11. Comparison of Nyquist plots for 0.88 mM H_2O_2, 0.10 M $NaClO_4$, 1) -0.28 V 2) -0.25 V; for 0.88 mM H_2O_2, 0.10 M Na_2SO_4, 3) -0.28 V 4) -0.25 V

3.3.4. Influence of pH

The impedance data for 88 mM H_2O_2 in 0.10 M NaCl at different pH are shown in Figure 12. The pH was adjusted with dilute HCl or NaOH. When the data were compared at the same potential, the impedance curve was smoother and the values were less at higher pH indicating better electronic character. There was no significant difference in the frequency at which the real impedance became negative.

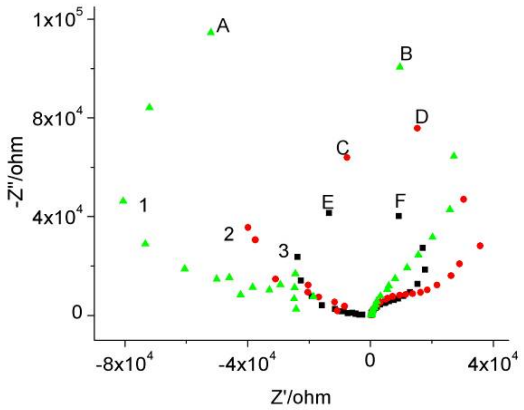

Figure 12. Nyquist plot for 0.1M NaCl, 88 mM H_2O_2, -0.28 V, 1) pH 3.05 2) pH 5.26 5) pH 9.28; Frequency at points A) 1.350 Hz B) 1.745 Hz C) 0.628 Hz D) 0.811 Hz E) 2.244 Hz F) 2.899 Hz; The real impedance became negative at points A, C, and E

3.3.5. Impedance in basic solutions and influence of added chloride

We have investigated the impedance behavior of H_2O_2 in 0.04 M NaOH to assess the influence of OH^- ions only. Since two new chloride induced oscillations have been reported in acidic solutions of peroxide, we have also investigated the influence of 1 and 2 mM NaCl in 0.04 M NaOH and 88 mM H_2O_2. These results are included in Figures 13a, 13b, and 13c. In these highly basic solutions we noticed much higher H_2O_2 decomposition at the platinum counter electrode and attributed the variations in results observed with repeated measurements, as shown in Figures 13b and 13c, as due to this decomposition. Such variations were not observed in near neutral as well as in acidic solutions.

Based on our results in Figure 13 c with 1mM and 2 mM NaCl in 0.04 M NaOH and 88 mM H_2O_2, the influence of chloride was not significant in basic solutions. The nature of the impedance spectra was similar in the absence and presence of chloride. Chloride seemed to make the electronic process a little more efficient based on the slight decrease in impedance. The frequency at which the real impedance became negative was not affected under the present set of concentrations studied. We had noticed a slight increase in the cathodic current both during the forward and reverse scans in the region of 'activated' or 'autocatalytic' reduction of H_2O_2 [28]

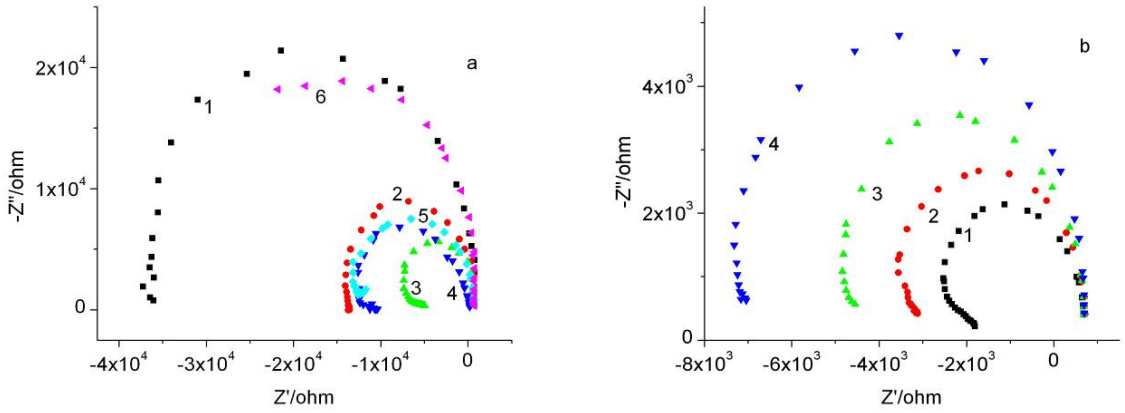

Figures 13a, 13b Nyquist plot for 88 mM H_2O_2 in 0.04 M NaOH at a) 1) -0.37 V 2) -0.34 V 3) -0.30 V 4) -0.28 V 5) -0.25 V 6) -0.22 V; Negative real impedance was observed at frequencies 1) 49.3 Hz 2) 78.9 Hz 3) 98.6 Hz 4) 262.9 Hz 5) 98.6 Hz 6) 28.26 Hz ; b) stability of results for 4 sets of data at -0.30 V. Negative real impedance was observed at frequencies: 1) 157.7 Hz 2) 157.7 Hz 3) 157.7 Hz 4) 131.4 Hz

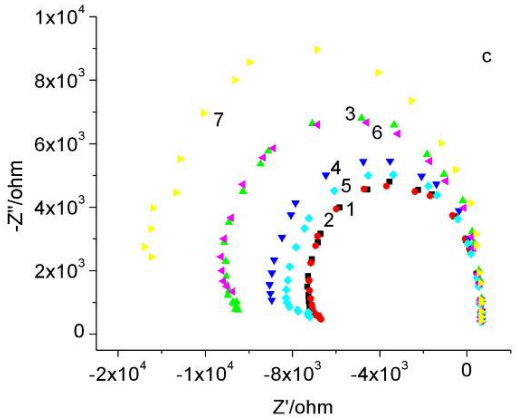

Figure 13c Nyquist plot at -0.3 V for 88 mM H_2O_2 and 0.04 M NaOH and 1) 0 M NaCl, 2,3 and 4) 1 mM NaCl, 5,6,7) 2 mM NaCl; Negative real impedance was observed at frequencies: 1) 131.4 Hz 2) 131.4 Hz 3) 98.6 Hz 4) 98.6 Hz 5) 98.6 Hz 6) 98.6 Hz 7) 78.9 Hz

3.4. Semiconduction

Polarization of metals at various potentials produces passive films. Many of these passive films produced on metals and alloys exhibit properties of an inner p-type oxide layer and an outer n-type hydroxide layer with a p-n heterojunction [30, 31]. The space charge region of these semiconductive passive films is often characterized by carefully evaluating the capacitance, C.

$$C = - 1/(\omega Z'') \quad (1)$$

If the capacitance of the Helmholtz layer is large compared to that of the space charge region, then the characteristic space charge capacitance of these semiconducting films obeys the Mott-Schottky relationship that connects C of a p-type semiconductor and the electrode potential E:

$$C^{-2} = -[2/(q\varepsilon\ \varepsilon_0 N_A)]\ (E-E_{FB} + kT/q) \qquad (2)$$

where ε is the vacuum permittivity (8.85 x 10^{-14} F/cm), ε_0 the dielectric constant of the specimen, q the electron charge (1.602 x 10^{-19} Coulomb), k the Boltzmann constant (1.38 x 10^{-23} J/K), T the absolute temperature, N_A the acceptor density, and E_{FB} the flat band potential. The intercept on the potential axis gives the flat band potential. The slope is inversely proportional to the doping concentration and can be obtained provided the dielectric constant of the passive film is known.

The Mott-Schottky plots for 88 mM H_2O_2 in 0.01 M NaCl are shown in Figure 14. Different flat band potentials for Cl^-, Br^-, and I^- [32] suggested that it was not just the oxide and hydroxide layers responsible for the observed phenomena. Instead, the highly insoluble mercurous ion halide complex might be involved in the formation of the film. In the case of aqueous NaCl, we had observed a narrow transition region with spectacular phase behavior and impedance loci with negative differential resistance [33].

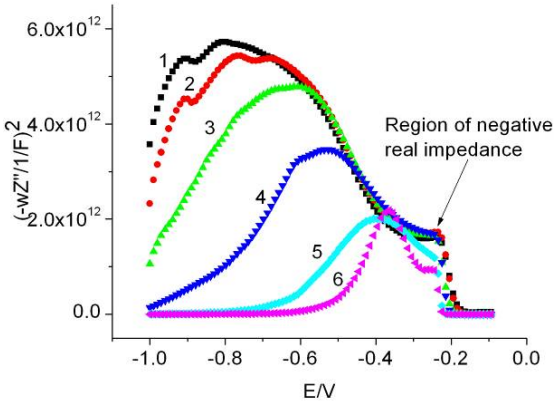

Figure 14. Mott-Schottky plot of 88 mM H_2O_2 in 0.10 M NaCl containing, pH 5.25, 1) 1000 Hz 2) 750 Hz 3) 500 Hz 4) 250 Hz 5) 100 Hz 6) 50 Hz

The potential region where negative real impedance was observed with mercury in aqueous NaCl was close to the passivation region and this was where the Mott-Schottky plot line intercepted the potential axis, or close to the flat band potential. This was different for the H_2O_2 system observed in our present experiments. The region where we had observed the negative real impedance was the region where there was an increase in the cathodic current on scanning from the most negative potential in the positive direction in cyclic voltammetry.

3.5. Stability of Experimental Data

We have checked the reproducibility of the impedance data and the results for 4 sets of data are shown in Figures 15 a, 15b, and 15c. At this potential, in the region of 'activated' or 'autocatalytic' H_2O_2 reduction region, several complex reactions are taking place. Also some decomposition of the H_2O_2 took place at the platinum counter electrode. There was also a slight increase in pH after 2 or 3 hours of different measurements. In spite of that, the consistency observed in these data was excellent.

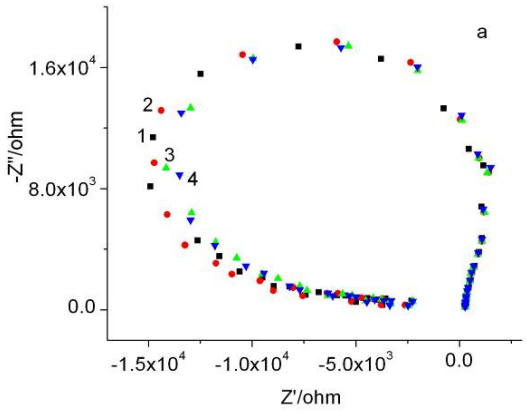

Figure 15a Stability of Nyquist plot for 88 mM H_2O_2 in 0.10 M NaCl, pH ~ 6.0, -0.28 V, 4 sets of data

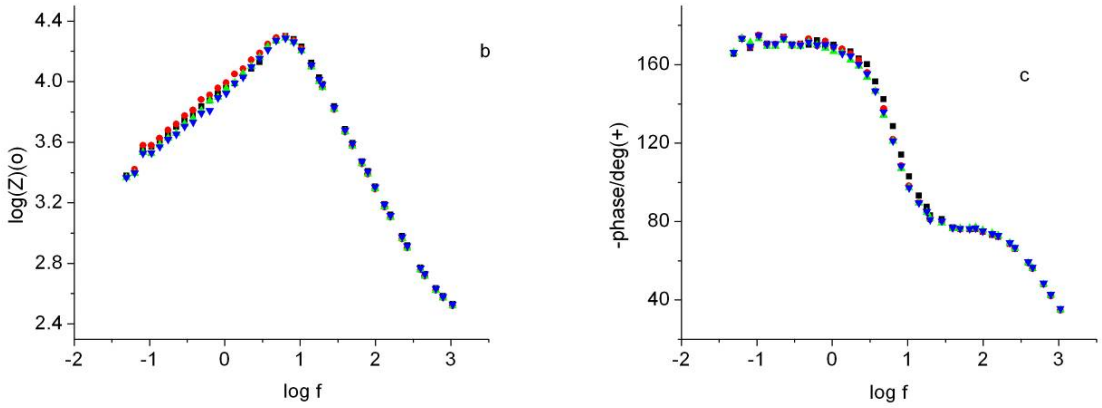

Figure 15b, 15c Stability of 0.10 M NaCl containing 88 mM H_2O_2 in 0.10 M NaCl, pH ~ 6.0, -0.28 V, b, Modulus of impedance; c, Phase angle, 4 sets of data

We have noticed more variability in the impedance data in highly basic solutions and these are discussed in section 3.3.4

3.6. Surface Area

The advantage of using the mercury working electrode is that one can get a fresh drop of clean mercury with almost no inhomogeneities. Also the surface area can be easily changed by changing the size of the mercury drop. The impedance data for 88 mM H_2O_2 in 0.10 M NaCl as a function of surface area are given in Figure 16. It was clear that the electronic process, as evidenced by impedance in 2 quadrants with negative real impedance, became more efficient with increasing surface area.

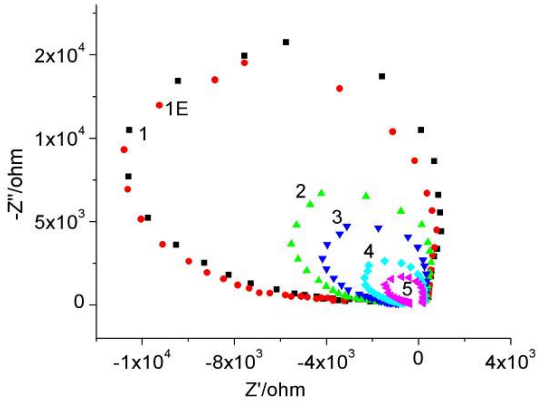

Figure 16. Influence of surface area on the impedance of 0.10 M NaCl containing 0.3% H_2O_2, pH ~ 6.0, -0.28 V, Nyquist plot, surface area, cm^2:1) 0.011 2) 0.017 3) 0.022 4) 0.031 5) 0.039 1E) 0.011 repeat at the end of all other measurements.

4. OSCILLATIONS IN ACIDIC AND BASIC SOLUTIONS OF H_2O_2

All living systems exhibit dynamical spatiotemporal periodicities [34]. The dynamical oscillations observed in the electrochemical passivation of metals and used as models for biological oscillations are attributed to the negative Faradaic impedance characteristics of the electrode [35]. Impedance data provide information on the instabilities or bifurcations and distinguish between saddle-node and Hopf bifurcations. A number of electrochemical oscillations have been reported in recent reviews [35-42]. We are particularly interested in the numerous H_2O_2 oscillations reported in acidic and basic solutions [17-26, 43-47] and in attempts to classify electrochemical oscillations [37, 48-49]. We have also reported the impedance behavior of several simple biological molecules that exhibit impedance loci in several quadrants [50].

The complexity of the H_2O_2 system can be recognized from the fact that five oscillations, A-E, have been reported for H_2O_2 on Pt electrode in acidic solutions [46, 47]. Oscillation A observed in the potential region just before hydrogen evolution and oscillation E observed only on single crystal Pt (111) electrode are classified as NDR (negative differential resistance) oscillators. Oscillations C and D observed in the presence of small amounts of halide ions are classified as HNDR (hidden negative differential resistance) oscillators (negative differential resistance in a region of intermediate frequencies and positive differential resistances at low frequencies). Oscillation B occurring at more cathodic potentials is classified as a coupled NDR (HNDR) oscillator. The autocatalytic effect of adsorbed OH (as an NDR inducing species for oscillation E) on the dissociative adsorption of H_2O_2, the catalytic effect of adsorbed halogen, the formation of under-potential deposited hydrogen (upd-H) (as an NDR inducing species for oscillation A) just before hydrogen evolution, and another type of adsorbed hydrogen called, “on top H”, that produces hydrogen have been incorporated in explaining the different oscillations. The reactions employed to describe some of these processes include [46]:

$$2Pt + H_2O_2 \rightarrow 2Pt\text{-}OH \quad (3)$$

$$Pt\text{-}OH + H^+ + e^- \rightarrow Pt + H_2O \quad (4)$$

$$2Pt\text{-}OH \rightarrow 2Pt + O_2 + 2H^+ + 2e^- \quad (5)$$

$$4Pt\text{-}OH \rightarrow 4Pt + O_2 + 2H_2O \quad (6)$$

$$Pt + H^+ + e^- \rightarrow Pt\text{-}H \text{ (upd-H)} \quad (7)$$

$$Pt + H^+ + e^- \rightarrow Pt\text{-}H \text{ (on-top-H)} \quad (8)$$

$$Pt\text{-}H \text{ (on-top-H)} + Pt\text{-}H \text{ (on-top-H)} \rightarrow 2Pt + H_2 \quad (9)$$

It must be pointed out that most investigations are based on current vs. potential curves under potential or current controlled conditions and not on impedance data. On the other hand we have focused our efforts mostly on impedance spectra. While we had observed current oscillations in cyclic voltammetric data in highly basic solutions only, we have observed negative differential resistance in all cases except in 0.10 M HCl.

We have focused our attention on the oscillation or impedance behavior of H_2O_2 from a biological point of view. This requires the presence of electrolytes such as NaCl or Na_2SO_4 around neutral pH. The data in Figure 9 suggest that it may be possible to have still lower concentrations of H_2O_2 and observe impedance in two quadrants or negative differential resistance, which is a characteristic of tunnel diode behavior. Considering the fact that the H_2O_2 concentration in biological systems is less than 1 mM except when a burst release is observed, its influence in controlling the electronic processes such as cell signaling is quite significant. A comparison of the data in Figures 6-10, suggest the symmetry of the electronic process, which depends on the electrolyte concentration, peroxide concentration, pH, the anion, and the applied potential. The circuit that could be effective under a variety of conditions makes the treatment of Parkinson's disease by deep brain stimulation quite challenging.

5. ELECTROCHEMISTRY OF H_2O_2 IN AQUEOUS NaCl AND DEEP BRAIN STIMULATION TREATMENT OF PARKINSON'S DISEASE

Hydrogen peroxide diffuses readily through cell membranes. It decomposes in the presence of transition metals to the highly reactive hydroxyl radical, as exemplified by reaction 13. This radical is the cause of most of the oxidative damage to proteins, lipids, sugars, and nucleic acids, by way of two major reactions, hydrogen abstraction and addition [51]. Hydrogen peroxide acts as an important signaling molecule. It can also activate an important transcription factor, NF-kB, involved in inflammatory responses [51]. While at low concentrations, H_2O_2 serves as an intracellular messenger and stimulates cell proliferation, at higher concentrations and on prolonged exposure, H_2O_2 induces cell death by both apoptosis and necrosis.

In the preceding paper, we have reported the involvement of more than 30 reactions in describing the electrochemistry of H_2O_2. This molecule can be an oxidizing agent or reducing agent depending on the nature of other substrates and the acidity of the solution. It can also disproportionate to produce oxygen and water.

Progressive reduction of O_2 produces $O_2^{\cdot -}$, H_2O_2, and finally $^{\cdot}OH$ along with OH^-.

$$O_2 + e^- \rightarrow O_2^{\cdot -} \quad (10)$$
$$O_2^{\cdot -} + e^- + 2H^+ \rightarrow H_2O_2 \quad (11)$$
$$H_2O_2 + e^- \rightarrow {}^{\cdot}OH + OH^- \quad (12)$$

The hydroxyl radical can lead to lipid peroxidation and alter the structural integrity of neural membranes. Excess Fe^{2+}, also found in patients with Parkinson's disease, can reduce peroxide and produce $^{\cdot}OH$.

$$H_2O_2 + Fe^{2+} \rightarrow {}^{\cdot}OH + OH^- + Fe^{3+} \quad (13)$$

Dopamine undergoes auto-oxidation, producing $O_2^{\cdot -}$, H_2O_2, semiquinone radical and finally a quinone [1].

$$\text{Dopamine} + O_2 \rightarrow \text{Semiquinone}^{\cdot} + O_2^{\cdot -} + H^+ \quad (14)$$
$$\text{Dopamine} + O_2^{\cdot -} + H^+ \rightarrow \text{Semiquinone}^{\cdot} + H_2O_2 \quad (15)$$
$$\text{Semiquinone}^{\cdot} + O_2 \rightarrow \text{Quinone} + O_2^{\cdot -} + H^+ \quad (16)$$

Hydrogen peroxide is also produced when dopamine is metabolized enzymatically by monoamine oxidase [1].

$$\text{Dopamine} + O_2 + H_2O \rightarrow \text{3,4 Dihydroxyphenylacetaldehyde} + NH_3 + H_2O_2 \quad (17)$$

Neurostimulator implants used for treating Parkinson's disease deliver electrical impulses to the brain and block abnormal nerve signals caused by substantial reductions of nigral dopaminergic neurons and striatal dopamine concentration. The pulse generator used for this treatment by deep brain stimulation of the thalamic ventral intermediate nucleus can control different variables of stimulation, such as contact (cathode or anode), voltage (0 to 10.5 V), rate (2 to 185 Hz), pulse width (60 to 450 μsec) and timing (cyclic or continuous stimulation) [15].

Our impedance results have shown that the negative differential resistance, often characterized by impedance loci occurring in the first and second quadrants, is also a characteristic of the tunnel diode behavior. This impedance behavior of H_2O_2 is sensitive to pH, bulk electrolyte concentration, concentration of H_2O_2, and the applied potential. Depending on the concentration of the peroxide and the electrolyte, the impedance behavior can be very smooth or somewhat chaotic. The frequency at which the real impedance becomes negative depends on the applied potential, concentration of H_2O_2 and the bulk electrolyte concentration. We have observed negative real impedance in the frequency range 260 Hz – 40 mHz. This is comparable to that used to treat Parkinson's disease by deep brain stimulation. Thus the need to control several variables, mentioned earlier, can be understood because it may be trying to counteract the complexity of the electronic circuits produced by varying concentrations of H_2O_2 produced in the brain at different times and at different locations.

6. CONCLUSIONS

Oxidative stress, due to excessive reactive oxygen species such as H_2O_2, is implicated in the pathogenesis of Parkinson's disease. We have investigated the electronic behavior of this molecule in the presence of the most common biological electrolyte, sodium chloride, by frequency response analysis. H_2O_2 exhibited negative differential resistance or impedance in the first and second quadrants, a characteristic of tunnel diode behavior. With increasing concentration of H_2O_2, there was a shift to slightly more negative potentials at which the impedance spectra exhibited negative real impedance. This was in agreement with the observation of a slight cathodic shift in the cyclic voltammetric peak. When the potential was changed from the most cathodic to less and less cathodic, the impedance spectral characteristics changed from capacitive loops to impedance in two quadrants and then back to capacitive loops. In the range of potentials at which negative differential resistance was observed, there was a fixed potential at which the frequency was the highest when the impedance became negative. At this potential, the higher the H_2O_2 concentration, the higher the frequency at which the real part of the impedance became negative. Depending on the potential and concentration of H_2O_2, negative real impedance was observed at frequencies in the range 260 Hz – a 40 mHz. The variations in impedance data were higher in 0.04 M NaOH compared to that in near neutral solutions. We had observed insignificant influence of 1 or 2 mM chloride on the impedance spectra in highly basic solution. Negative differential resistance was also observed for 88 mM H_2O_2 in solutions of 0.10 M $NaClO_4$ and 0.10 M Na_2SO_4.Our results suggest that the electronic character of H_2O_2 is dictated by the potential, bulk electrolyte concentration, pH, and the concentration of H_2O_2. To explain our admittance data, we have introduced the concept of "potential induced and peroxide-mediated" ion pair formation between sodium and chloride ions in a way similar to the "potential induced and water-structure-enforced" ion pair formation. Our results demonstrate the need for multiple electrodes at multiple locations with tunable frequencies and voltages for treatment of Parkinson's disease by deep brain stimulation because of the variations in the concentration of H_2O_2 at different locations and at different times and consequent subtle changes in its electronic properties.

ACKNOWLEDGEMENT
Benjamin Chu gratefully acknowledges partial support of this work provided by the Basic Energy Sciences, Department of Energy (DEFG0286ER45237)

References

1. C.W. Olanow and A.N. Lieberman Editors in, *"The Scientific Basis for the Treatment of Parkinson's Disease"*, The Parthenon Publishing Group, New Jersey, 07656, USA, (1992)
2. W.J. Weiner, L.M. Shulman, A.E. Lang, *"Parkinson's Disease"*, 2nd ed., The John Hopkins University, Maryland, USA (2007)
3. A.E. Lang, A.M. Lozano, *N. Eng. J. Med.,* 339 (1998) 1044
4. A.E. Lang, A.M. Lozano, *N. Eng. J. Med.,* 339 (1998) 1130
5. J.B. Martin, *N. Eng. J. Med.,* 340 (1999) 1970
6. K.N. Prasad, W.C. Cole, B. Kumar, *J. Am. College of Nutrition,* 18 (1999) 413

7. D. Chiu, B. Lubin, S.B. Shoket, *Free Radicals in Biology* (A.W. Pryor, eds.), Academic Press, New York, NY, USA, (1982) 115
8. A. Starkov, K.B. Wallace, in "*Oxidative Stress, Disease and Cancer"*, Keshav K. Sing ed., Imperial College Press, London, 1 (2006)
9. G. Lenaz, C. Bovina, M. D'Aurelio, R. Fato, G. Formiggini, M.I. Geneva, G. Giulianao, P.M. Merb, Parestica Ventura B, *Ann. NY Acad. Sc.,* 959 (2002) 199
10. Y. Liu, G. Fiskum, O. Schubert O, *J. Neurochem.,* 80, (2002) 780
11. Q. Chen, E.J. Vasquez, S. Moghaddas, C.L. Hoppel, E.J. Lesnefsky, *J. Biol. Chem.,* 278 (2003) 36027
12. V.M. Mann, J.M. Cooper, D. Frige, S.E. Daniel, A.H. Schapira, C.D. Marsden, *Brain,* 115 (1992) 33
13. T.M. Hagen, J. Liu, J. Lykkesfeldt, C.M. Wehr, R.T. Ingersoll, V. Vinarsky, J.C. Bartholomew, B.N. Ames, *Proc. Natl. Acad. Sc. USA,* 99 (2002) 1870
14. C. Haberler, F. Alesch, P.R. Mazal, P. Pilz, K. Jellinger, M.M. Pinter, J.A., Hainfellner, H. Budka, *Annals of Neurology,* 48 (2000) 372
15. P. Limousin, P. Krack, P. Pollack, A. Benazzouz, C. Ardouin, D. Hoffmann, A.L. Benabid, *N. Eng. J. Med.,* 339 (1998) 1105
16. B.S. van Asbeck, R.C. Sprong, T. van der Bruggen, J.F.L.M. van Oirschot, J.C.C. Borleffs in *"Oxidative Stress in Cancer, Aids, and Neurodegenerative Diseases"*, L. Montagnier, R. Olivier, and C. Pasquier, editors, CRC Press, Taylor & Francis Group, New York, (1998) 97
17. S. Fukushima, S. Nakanishi, K. Fukami, S. Sakai, T. Nagai, T. Tada, Y. Nakato, *Electrochemistry Communications*, 7 (2005) 411 and references therein
18. Y. Mukouyama, S. Nakanishi, H. Konishi, Y. Ikeshima, Y. Nakato, *J. Phys. Chem*., B 105 (2001) 10905
19. M. T. M. Koper, A. M. Chaparro, H. Tributsch, D. Vanmaekelbergh, *Langmuir*, 14 (1998) 3926 and references therein.
20. G. Flätgen, S. Wasle, M. Lübke, C. Eickes, G. Radhakrishnan, K. Doblhofer, G. Ertl, *Electrochimica Acta*, 44 (1999) 4499
21. J. J. Lingane, P. J. Lingane, *J. Electroanal. Chem*., 5 (1963) 411
22. G. Neher, L. Pohlmann, H. Tributsch, *J. Phys. Chem.,* 99 (1995) 17763
23. S. Cattarin, H. Tributsch, *Electrochimica Acta,* 38 (1993) 115
24. S. Štrbac, R. R. Adžić, *J. Electroanal. Chem*., 337 (1992) 355
25. M.V. Vazquez, S.R. de Sanchez, E.J. Calvo, D.J. Schiffrin, *J. Electroanal. Chem*., 374 (1994) 179
26. M. Honda, T. Kodera, H. Kita, *Electrochimica Acta*, 28 (1983) 727
27. C.V. Krishnan, M. Garnett, B. Chu, *Int. J. Electrochem. Sci.,* 2 (2007) 958
28. C.V. Krishnan, M. Garnett, B. Chu, *Int. J. Electrochem. Sci.,* 3 (2008) 1348
29. F.A. Cotton, G. Wilkinson, "*Advanced Inorganic Chemistry*", 3rd edition, Interscience Publishers, New York, (1972) 415
30. H. Tsuchiya, S. Fujimoto, T. Shibata, *J. Electrochem. Soc.,* 151 (2004) B39 and references therein
31. D.S. Kong, S.H.Chen, C. Wang, W. Yang, *Corrosion Science,* 45 (2003) 747 and references therein
32. C. V. Krishnan, M. Garnett, *Electrochimica Acta,* 51 (2006) 1541
33. C.V. Krishnan, M. Garnett, B. Chu, *Int. J. Electrochem. Sci.,* 3 (2008) 1127
34. R. J. Field and L. Gyorgyi, Editors in *"Chaos in Chemistry and Biochemistry",* World Scientific Publishing Co., NJ 07661, USA, (1993)
35. M. T. M. Koper, *Adv. Chem. Phys*., 92 (1996) 161
36. J. L. Hudson and T. T. Tsotsis, *Chem. Eng. Sci*., 49 (1994) 1493
37. K. Krischer, in *Modern Aspects of Electrochemistry*, B. E. Conway, J. O'M. Bockris, R. E. White, Editors, p.1, Plenum, New York, 32 (1999) 1
38. K. Krischer, N. Mazouz, and P. Grauel, *Angew. Chem, Int. Ed*., 40 (2001) 850

39. P. Strasser, *Electrochem. Soc. Interface*, 9 (2000) 46
40. J. Ross, M. Schell, *Ann. Rev. Biophys. Biophys. Chem.,* 16 (1987) 401
41. T.Z. Fahidy, Z.H. Gu, in *"Modern Aspects of Electrochemistry"*, R.E. White, J.O'M. Bockris, B.E. Conway, Editors, 27 (1995) 383
42. H. Hommura, Y. Mukouyama, T. Matsuda, S. Yae, Y. Nakato, *Chem. Letters,* (1996) 391
43. T.G.J. van Voorji, M.T.M. Koper, *Electrochim. Acta,* 40 (1995) 1689
44. Y. Mukouyama, S. Nakanishi, Y. Nakato, *Bull. Chem. Soc. Jpn.,* 72 (1999) 2573
45. Y. Mukouyama, S. Nakanishi, K. Karasumi, A. Imanishi, N. Furuya, H. Konishi,Y. Nakato, *J. Phys. Chem.*, B 104 (2000) 4181
46. Y. Mukouyama, S. Nakanishi, H. Konishi,K. Karasumi, Y. Nakato, *Phys. Chem. Chem. Phys.,* 3 (2001) 3284
47. Y. Mukouyama, S. Nakanishi, T. Chiba, K. Murakoshi, Y. Nakato, *J. Phys. Chem.,* B105 (2001) 7246
48. P. Strasser, M. Eiswirth, and M. T. M. Koper, *J. Electroanal. Chem*., 478 (1999) 50
49. M.T.M. Koper, *J. Electroanal. Chem*., 409 (1996) 175
50. C.V. Krishnan, M. Garnett, in *Passivation of Metals and Semiconductors, and Properties of Thin Oxide Layers*, P. Marcus and V. Maurice, Editors, Elsevier, Amsterdam, (2006) 389
51. C.D. Berdanier, in *"Mitochondria in Health and Disease"*, CRC Press, Taylor and Francis Group, New York Boca Raton, Florida, USA, (2005)